

# Comparison of morphology, orientation, and migration of tendon derived fibroblasts and bone marrow stromal cells on electrochemically aligned collagen constructs

Umut Atakan Gurkan,<sup>1</sup> Xingguo Cheng,<sup>2\*</sup> Vipul Kishore,<sup>1\*</sup> Jorge Alfredo Uquillas,<sup>1</sup> Ozan Akkus<sup>1</sup>

<sup>1</sup>Weldon School of Biomedical Engineering, Purdue University, 206 S. Martin Jischke Drive, West Lafayette, Indiana 47907-2032

<sup>2</sup>Biomedical Material Engineering, Division 01 Southwest Research Institute, San Antonio, Texas 78238

Received 13 November 2008; revised 20 October 2009; accepted 26 January 2010

Published online 31 March 2010 in Wiley InterScience ([www.interscience.wiley.com](http://www.interscience.wiley.com)). DOI: 10.1002/jbm.a.32783

**Abstract:** There are approximately 33 million injuries involving musculoskeletal tissues (including tendons and ligaments) every year in the United States. In certain cases the tendons and ligaments are damaged irreversibly and require replacements that possess the natural functional properties of these tissues. As a biomaterial, collagen has been a key ingredient in tissue engineering scaffolds. The application range of collagen in tissue engineering would be greatly broadened if the assembly process could be better controlled to facilitate the synthesis of dense, oriented tissue-like constructs. An electrochemical method has recently been developed in our laboratory to form highly oriented and densely packed collagen bundles with mechanical strength approaching that of tendons. However, there is limited information whether this electrochemically aligned collagen bundle (ELAC) presents advantages over randomly oriented bundles

in terms of cell response. Therefore, the current study aimed to assess the biocompatibility of the collagen bundles *in vitro*, and compare tendon-derived fibroblasts (TDFs) and bone marrow stromal cells (MSCs) in terms of their ability to populate and migrate on the single and braided ELAC bundles. The results indicated that the ELAC was not cytotoxic; both cell types were able to populate and migrate on the ELAC bundles more efficiently than that observed for random collagen bundles. The braided ELAC constructs were efficiently populated by both TDFs and MSCs *in vitro*. Therefore, both TDFs and MSCs can be used with the ELAC bundles for tissue engineering purposes. © 2010 Wiley Periodicals, Inc. *J Biomed Mater Res Part A*: 94A: 1070–1079, 2010.

**Key Words:** tendon, ligament, biocompatibility, tissue engineering, cell migration

## INTRODUCTION

Soft tissue injuries are a major clinical problem worldwide.<sup>1</sup> Nearly 33 million Americans suffer musculoskeletal injuries every year,<sup>2</sup> costing an estimated \$30 billion.<sup>3</sup> In the specific case of tendons, the causes of injury are several: laceration, contusion, sport injuries, or repetitive motion.<sup>4,5</sup> The natural process of healing includes three well-defined and overlapping phases: homeostasis with inflammation, proliferation with fibroplasia, and remodeling with maturation.<sup>4,6</sup> However, the outcome of this healing process varies greatly among patients and injury characteristics,<sup>7–9</sup> and is generally unsuccessful to restore tendon's functional capability to bear daily loads.

Suturing is the current standard to repair and replace damaged tendons.<sup>10</sup> A major limitation of this technique is the weak points generated by the suture knots at the repair site. Autografts are considered to be another alternative for tendon repair and reconstruction. However, they are limited in supply and may result in donor site morbidity.<sup>11</sup> Allografts<sup>12,13</sup> or xenografts<sup>14,15</sup> are inferior to autografts as the material strength is compromised during harvest, processing and sterilization. The risk of disease transmission, while

being low, is still a concern for allografts.<sup>16</sup> Tissue engineering offers a promising alternative approach for tendon/ligament repair by combining biodegradable biomaterials seeded with appropriate cell sources. Due to structural and biochemical characteristics, good biocompatibility and cell adhesion properties, Type I collagen has been investigated as a good natural biomaterial for tendon repair.<sup>17–20</sup> Cell-collagen constructs have been shown to significantly improve the repair over natural healing<sup>21,22</sup>. Although, even after crosslinking, randomly oriented collagen is mechanically weak due to lack of alignment and packing density. Recently, we developed a novel electrochemical process to align the collagen molecules into highly oriented and densely packed fiber bundles.<sup>23</sup> After crosslinking with a natural and biocompatible crosslinking agent (genipin), the mechanical strength of the electrochemically aligned collagen (ELAC) bundles was about 40 MPa, a value which converges upon that of natural tendon (canine tendon strength has been reported to be about 80 MPa).<sup>23</sup>

Two cell resources have been widely proposed and tested for tendon repair via tissue engineering: tendon-derived fibroblasts (TDFs) and bone marrow stromal cells

\*These authors contributed equally to this work.

Correspondence to: O. Akkus; e-mail: ozan@purdue.edu

Contract grant sponsor: National Institutes of Health; contract grant number: NIH 1R21AR056060

Contract grant sponsor: National Science Foundation (CBET division); contract grant number: 0754442

(MSCs).<sup>22,24,25</sup> These two cell types are pertinent to tendon repair as they can originate and populate implanted constructs from nearby bone tissues as well as remnants of host tendon which needs to be reconstructed. However, there is limited knowledge on the response of these two cell types to the newly developed genipin crosslinked ELAC bundles. In an effort to address this limitation, the aims of this study were: (1) to assess the biodegradability and the cytotoxicity of ELAC; (2) to investigate the migration and population of TDFs and MSCs on single ELAC and genipin crosslinked random (CX-Random) bundles *in vitro*; (3) to confirm that the MSCs do not undergo nonspecific differentiation (osteogenic) on ELAC bundles; (4) to quantitatively compare the cytoskeletal alignment of the MSCs and the TDFs on ELAC and CX-Random bundles; (5) to assess the ability of MSCs and TDFs to populate 3D constructs fabricated by braiding multiple ELAC bundles.

## MATERIALS AND METHODS

### Preparation of ELAC bundles, CX-Random bundles and 3D ELAC constructs

ELAC bundles were prepared as previously described.<sup>23</sup> Briefly, acid-soluble monomeric collagen solution was dialyzed (Nutrigen, 6 mg/mL; Advanced Biomatrix, San Diego, CA) and loaded between two parallel wire electrodes. Following the application of electric current to the solution, collagen molecules in the solution between the electrodes align, migrate and pack into a collagen bundle.<sup>23</sup> Freshly prepared bundles were incubated in 10X Phosphate Buffer Saline (PBS, pH 7.4, 37°C) solution for 12 h to improve the hierarchical structural organization of the ELAC bundles by promoting D-banding pattern.<sup>26</sup> Next ELAC bundles were crosslinked in 15 mL of 0.625% genipin (Wako Pure Chemical, Osaka, Japan) in sterile 1X PBS solution at 37°C for 3 days. The dimensions of these ELAC bundles varied in the range of 50–400 µm in diameter and up to 70 mm in length [Fig. 1(A)]. The diameter of an individual bundle approximately corresponds to that of a secondary fascicle in tendon's hierarchical organization.<sup>27</sup> Three dimensional constructs were made by manually braiding the ELAC bundles together. The bundles grouped together as such had macroscopic interbundle spaces that allow cell migration and population [Fig. 1(B)].

Crosslinked randomly oriented collagen bundles (CX-Random) were used as controls. They were prepared by mixing the same dialyzed monomeric collagen solution used for ELAC synthesis with 10X PBS, casting on a glass surface as a layer, and gelling at 37°C. After crosslinking with genipin under the same conditions as described above, strips were cut from this layer using fresh surgical blades and used as CX-Random bundles for the migration study.

### *In vitro* degradation study

The digest solution was a mixture (pH = 7.4), which contained 0.1M tris-base, 0.25M CaCl<sub>2</sub>, and 125 U/mL Type I collagenase (Sigma) from *Clostridium histolyticum*. ELAC bundles were immersed in the digest solution (1 mg/200 µL) and incubated on orbital shaker at 37°C at 100 rpm. At

the designated time points (days: 1, 7, 14, 21, and 28), the remaining ELAC bundles were taken out, washed, serially dehydrated and weighed with an ultra sensitive balance (UMX5 Comparator, 0.0001 mg Readability, Mettler Toledo). The bundles were immersed in freshly prepared digest solution and weight measurements were repeated similarly at the ensuing time points.

### Extraction and culture of bone marrow stromal cells (MSCs)

Rat bone marrow was extracted from the femurs of 2–3 months old male Long-Evans rats from Harlan immediately after they were sacrificed under the approval of Purdue Animal Care and Use Committee. The growth medium composed of DMEM (Sigma, D5546) supplemented with 10% FBS (Sigma, F6178), 2 mM L-Glutamine (Sigma, G7513), 60 U/mL Penicillin, 60 µg/mL Streptomycin (Invitrogen, 15140-122), and 1.5 µg/mL Fungizone (Gibco, 15290-018). The contents of the medullary cavities of the femurs were flushed with the growth media into a sterile culture plate. The media containing the cells were transferred to T75 flasks incubated at 37°C and 5% CO<sub>2</sub> for 4 days and the unattached cells and the debris were washed away. The attached cells were incubated up to 80–90% confluence [Fig. 1(C)] and subcultured four times before being used in the direct contact test and migration studies.

### Extraction and culture of tendon-derived fibroblasts (TDFs)

Achilles tendons of 2–3 months old male Long-Evans rats were harvested aseptically. The tendon cells were harvested from the mid section of the Achilles tendon, which is free of any muscle tissue, after carefully peeling off the epitenon layer. The tendons were sliced into two pieces, disbanded with a sterile scalpel and each piece was incubated in a six-well plate with the growth medium at 37°C and 5% CO<sub>2</sub>. The TDFs leaving the tendon fragments attached onto the tissue culture treated plastic and reached 80–90% confluence on the 7<sup>th</sup> day. Next, the tendon fragments were removed and the cells were incubated till 80–90% confluence after each passage. The cells displayed typical spindle-like morphology [Fig. 1(D)] and they were subcultured four times before being used for cell migration and population assays.

### Cytotoxicity test of ELAC bundles

The MSCs (passage-4) were seeded in a 12-well plate and incubated at 37°C and 5% CO<sub>2</sub> for 2 days before the ELAC bundles were placed in the wells containing the cells. The ELAC bundles were cut into 10 mm length, sterilized in 70% ethanol for 24 h, rinsed three times with 1X PBS and once with the growth medium before they were placed in four wells (four fibers per well). The cells in direct contact with the ELAC bundles and the controls (cells only) were incubated for an additional 24 h before the number of viable cells was measured with CellTiter 96 AQ (Promega) cell proliferation assay according to the previously described standard protocols.<sup>28</sup>

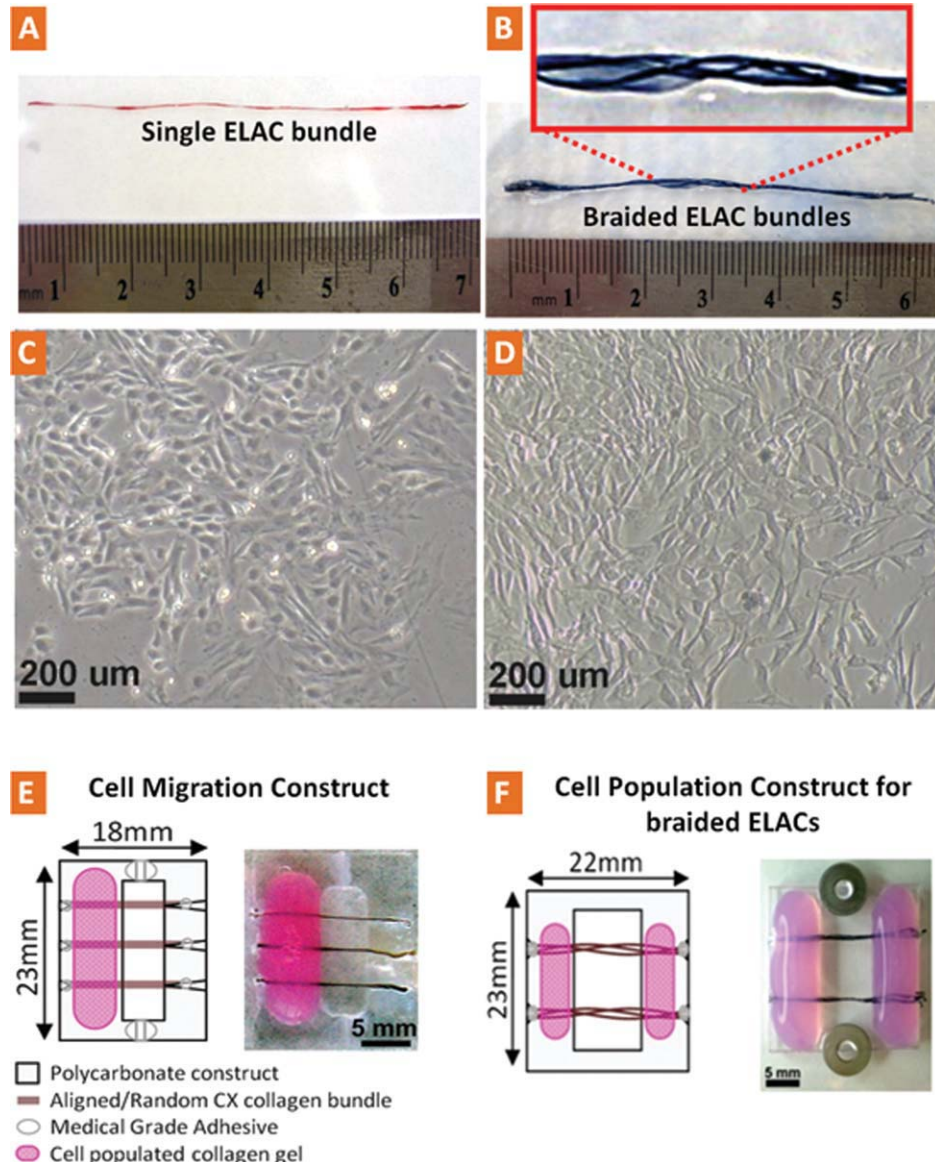


**FIGURE 1.** Photograph and schema of the collagen bundles, cells, cell migration, and cell population constructs. (A) Sirius red stained single ELAC bundle. (B) Multiple ELACs braided together to form a 3D construct. (C,D) Typical morphology of bone marrow stromal cells (MSCs, passage-3) and tendon-derived fibroblasts (TDFs, passage-3), respectively at about 90% confluence before being used in the migration and population studies. (E) Cell migration construct; cells were suspended in collagen gels (pink), which were loaded on polycarbonate substrate (gray). Cells were restricted to migrate out of the collagen gel onto the collagen bundle (brown) from one end to the other. (F) Cell population construct; cells were suspended in collagen gel (pink), which was loaded on both sides of the collagen bundles. Cells were able to migrate from both ends and populate on the 3D braided ELAC construct (brown). [Color figure can be viewed in the online issue, which is available at [www.interscience.wiley.com](http://www.interscience.wiley.com).]

#### Cell migration on single ELAC and CX-Random bundles

The cell migration assay used in this study was modified from Cornwell et al.<sup>29</sup> The constructs used in the assay were made out of 2 mm thick polycarbonate sheet and had a central gap, above which the ELAC bundles and CX-Random bundles were adhered to the constructs at the ends with medical grade adhesive (Loctite 4851) [Fig. 1(E)]. The adhesive had relatively high viscosity to minimize the wicking of the adhesive onto the collagen fibers. To prevent the cells from populating on the polycarbonate construct and reaching the far ends of the collagen fibers, vertical grooves

were machined on the upper and lower connecting polycarbonate sections [Fig. 1(E)]. These grooves were filled with a lower viscosity medical grade adhesive (Loctite 4014), which was confirmed to hinder the attachment of the cells drastically. The constructs were sterilized in 70% ethanol for 24 h and air dried in the laminar flow hood before seeding. The cells were seeded onto the construct in a Type I collagen gel lattice. The collagen gel was prepared by mixing eight parts Type I collagen (6 mg/mL) (Nutragen, USA) with 1 part 10X MEM (Sigma, M0275) and balancing the pH at 7.4 with 0.1N NaOH. A cell seeding density of  $1 \times 10^6$

cells/mL-gel was used for both cell types. The collagen gel containing the cells was then poured on the wider side of the air dried constructs [Fig. 1(E)] and incubated in CO<sub>2</sub>-free incubator for 45 min for gelation. After gelation, the growth media was added to the culture plates containing the migration constructs, sufficient to submerge the collagen fibers and the collagen gel lattice. Culture media changes were done twice per week. After incubation for 16 days, the constructs were taken out and the f-actin filaments of cell cytoskeleton were specifically stained with Fluorescein-Phalloidin (Molecular Probes) and imaged with fluorescent microscope (Olympus BX51) and confocal microscope (Olympus Fluoview 1000). The sample size for each group was in the range of  $n = 13\text{--}15$ .

#### **Quantification of the cytoskeletal alignment of MSCs and TDFs on ELAC and CX-Random bundles**

Image processing was conducted on f-actin stained images of MSCs and TDFs on ELAC and CX-Random bundles. Fluorescent images obtained from five individual samples for each material type (ELAC, CX-Random) and for each cell type (MSCs, TDFs) were converted to grayscale with Adobe Photoshop [Fig. 5(A)]. A built-in function (*edge*) in MATLAB Image processing toolbox was used to detect the edges of the individual fibers in the photographs with Canny filter method.<sup>30</sup> The fibrils oriented at angles between 1 and 90 degrees were counted with a built-in function (*imopen*) to morphologically open the images and evaluate the distribution of fibrils at various angles. To compare the alignment of the cells on different bundle types, the vertically oriented fibrils (along the long axis of the bundles) were counted and these numbers were statistically analyzed.

#### **Assessment of osteogenic activity of MSCs on ELAC and CX-Random bundles**

To investigate whether the MSCs undergo osteogenic differentiation on the ELAC and CX-Random bundles, alkaline phosphatase (AP) activity and Osteocalcin (OC) levels were measured at day-21 following the manufacturer's protocol. Briefly, the ELAC and CX-Random bundles covered with MSCs were washed with lysis buffer provided in the colorimetric *p*-Nitrophenyl phosphate (*p*NPP) substrate alkaline phosphatase assay kit (SensoLyteTM, Anaspec Corp., San Jose, CA). After washing, bundles were placed in the lysis buffer supplemented with triton-X 100, gently agitated at 4°C for 10 min, centrifuged at 2500×g for 10 min at 4°C and the supernatant was used for the osteogenic assays. Appropriate alkaline phosphatase standards were prepared to establish the calibration curve. Fifty microliter aliquots of samples and the standards were added to a 96-well plate followed by 50 μL *p*NPP substrate solution and incubated for 2 h at 37°C. The absorbance of the wells was measured at 405 nm with a plate reader (Molecular Devices, Spectra-max M5). Osteocalcin (OC) levels in the lysates were measured using a Rat Osteocalcin EIA kit (Biomedical Technologies, Stoughton, MA) in sensitive mode with the lowest detection limit of 0.5 ng/mL based on Maccarinelli et al.<sup>31</sup> Samples and standards (100 μL) were added to a 96-well

plate precoated with OC capture antibody, incubated for 20 h at 4°C and washed three times with phosphate-saline wash buffer. Following this, 100 μL of OC antiserum was added to each well, and incubated at 37°C for 1 h. Following another set of washes, 100 μL of diluted donkey anti-goat IgG peroxidase was added to each well and incubated for 1 h at room temperature. Hundred microliter of substrate mix (1:1 of hydrogen peroxide solution and tetramethyl benzidine) was then added and incubated at room temperature for 30 min. The reaction was stopped by adding 100 μL of stop solution to each well and the absorbance was measured using a microplate reader set at 450 nm with a wavelength correction set at 540 nm. Total protein amounts in the lysates were measured by using a bicinchoninic acid (BCA) protein assay kit (Pierce Protein Research Products). AP activity and OC levels were normalized by the total protein amount for each sample. MSCs cultured on regular tissue culture plastic for 21 days were included as a control group to quantify the baseline level of osteogenic activity of MSCs.

#### **Population of 3D ELAC constructs by MSCs and TDFs**

A similar migration construct as described above was used; however, to expedite migration towards the 3D bundles, the collagen gel acting as the cell source was poured on both sides [Fig. 1(F)]. The TDF-populated constructs were taken out on the 6<sup>th</sup> day while MSCs-populated construct were taken out on the 23<sup>rd</sup> day. Both constructs were stained and imaged similarly as described above. After 6 days of culture, the TDFs-ELAC constructs were fixed with 10% formalin, embedded in paraffin and stained with hematoxylin and eosin (H&E) for histological observation.

#### **Statistical analysis**

The results of the degradation study ( $n = 3$ ) were analyzed with one way ANOVA for repeated measures with Tukey post-hoc comparisons. The results of the direct contact cytotoxicity test ( $n = 4$ ) were evaluated by Mann-Whitney U test. TDF and MSC migration distances on ELAC and CX-Random bundles at 16 days ( $n = 13\text{--}15$ ) were analyzed using parametric General Linear Model with Tukey post-hoc test after checking the normality of the groups with Anderson-Darling normality test. AP activity ( $n = 8\text{--}12$ ), OC levels ( $n = 8\text{--}12$ ) and the number of vertically oriented fibers in different groups ( $n = 5$ ) was analyzed with Kruskal Wallis test followed by Mann-Whitney U test with Bonferroni correction for the number of comparisons. Statistical significance threshold was set at 0.05 for all tests (with  $p < 0.05$ ).

## **RESULTS**

#### ***In vitro* degradation study**

In the presence of collagenase (Type I), ELAC degraded in a nonlinear fashion over time [Fig. 2(A)]. After four weeks, about 28% of the original weight was observed to remain. The degradation was observed to take place on the surface of the densely packed ELAC as the bundles grew smaller in lateral dimensions.

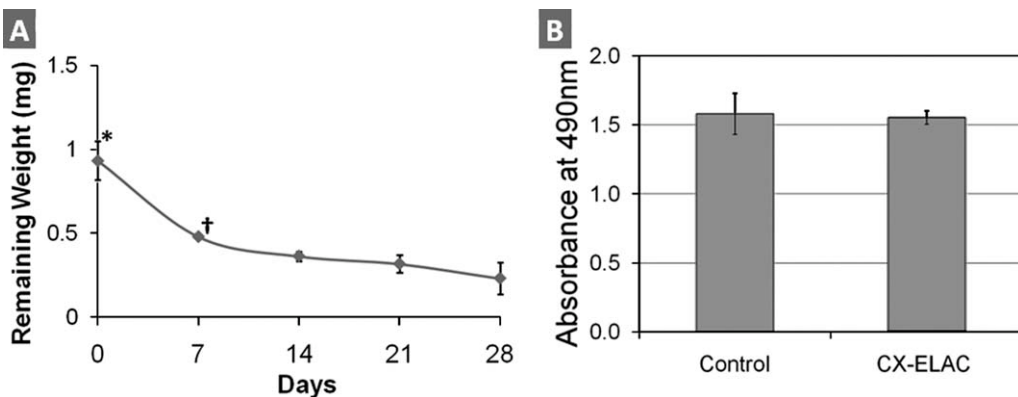


**FIGURE 2.** (A) *In vitro* degradation of ELAC bundles in the presence of bacteria collagenase Type I. Weight of remaining ELACs were plotted against different digestion time points (3 samples per time point). \* indicates significant difference ( $p < 0.05$ ) between day-0 and all the following time points (days 7, 14, 21, and 28). † indicates significant difference ( $p < 0.05$ ) between day-7 and days-21 and 28. Noncrosslinked collagen samples were completely degraded within 24 h (results not shown). (B) Direct contact test results of ELAC bundles for testing cytotoxicity. The number of viable cells (MSCs) after being exposed to ELAC bundles for 24 h corresponds to the absorbance measured at 490 nm by using Cell-Titer 96 AQ cell proliferation assay. There is no statistically significant difference in the number of viable cells between the experimental group and the control group ( $n = 4$ ,  $p > 0.05$ ), indicating that ELAC is not cytotoxic.

#### Cytotoxicity test of ELAC bundles

Direct contact test with four 10 mm long ELAC bundles indicated that the number of viable cells were not significantly different ( $p > 0.05$ ) than that of the control group without the ELAC bundles [Fig. 2(B)].

#### Migration of MSCs and TDFs on single ELAC and CX-Random bundles

MSCs were able to migrate and populate both the ELAC and CX-Random collagen bundles [Fig. 3(A,B)]. Within 16 days, MSCs migrated about 3.5 mm onto the ELAC bundles [Fig. 3(A)]. On the other hand, in the case of CX-Random, MSCs migrated up to 2 mm [Fig. 3(B)]. The migration distance of MSCs on ELAC was significantly greater than the migration distance of MSCs on CX-Random [Fig. 3(E)]. Similarly, TDFs migrated a significantly longer distance in 16 days on ELAC (about 8 mm) than on CX-Random (about 7 mm) [Fig. 3(C-E)]. In addition, the migration distance of TDFs on both ELAC and CX-Random was significantly greater compared to their MSC counterparts [Fig. 3(E)]. These results indicate that the ELAC is more receptive to cell migration compared to CX-Random collagen bundles.

#### Cytoskeletal alignment of MSCs and TDFs on ELAC and CX-Random bundles

High magnification confocal images of TDFs indicated that the stained F-actin filaments of the cell cytoskeleton are oriented along the collagen fibril direction of the ELAC [Fig. 4(A) and the inset]. On the other hand, the TDFs which migrated onto CX-Random bundles did not show a preferred orientation [Fig. 4(B)]. H&E stained histological sections of the TDF-populated ELAC indicated that the nuclei of the cells were elliptical with their major axes oriented along the fiber direction [Fig. 4(C)]. These observations were further analyzed through quantitative image processing of high magnification cytoskeletal images of MSCs and TDFs on

ELAC and CX-Random bundles (Fig. 5). The gray scale fluorescent images of the cytoskeletal f-actin filaments of MSCs and TDFs displayed orientation along the bundle long axis direction on the ELAC (vertical, 90°) and unorganized orientation on CX-Random [Fig. 5(A-C)]. The distribution of the fibers at angles between 1 and 90° displayed a high concentration between 70–80° and the highest concentration between 85 and 90° for both MSCs and TDFs on ELAC [Fig. 5(B)]. Both cell types on CX-Random displayed a broad distribution, concentrations being between 0–10°, 40–50°, 70–80°, and 85–90° [Fig. 5(B)]. The number of vertically oriented (along the bundle long axis direction, 90°) cytoskeletal filaments was significantly higher for TDFs on ELAC compared to TDFs on CX-Random and MSCs on ELAC. Additionally, MSCs on ELAC displayed a significantly higher number of vertically aligned fibers compared to MSCs on CX-Random. These results indicate that both cell types are more aligned on the ELAC compared to CX-Random collagen bundles.

#### Osteogenic activity of MSCs on ELAC and CX-Random bundles

The results of pNPP based AP-activity assay (normalized by total cellular protein) displayed no significant difference between the experimental groups of MSC-only (1.21 ng AP activity/μg protein, st. dev.: 0.38), MSCs on ELAC (1.58 ng AP activity/ug protein, st.dev.: 0.45) and MSCs on CX-Random (0.82 ng AP activity/ug protein, st.dev.: 0.21). The OC levels were not detectable in any of the three groups with the rat OC Enzyme Immuno Assay (EIA) kit in sensitive mode with the lowest detection limit of 0.5 ng/mL. The OC level of vitamin D stimulated osteoblastic cell cultures have been shown to be as high as 450 ng-OC/mg-protein, which is well above the detection limit of the OC EIA kit employed in this study.<sup>31</sup> These results indicate that MSCs on ELAC do not undergo osteogenic differentiation at the current culture conditions.

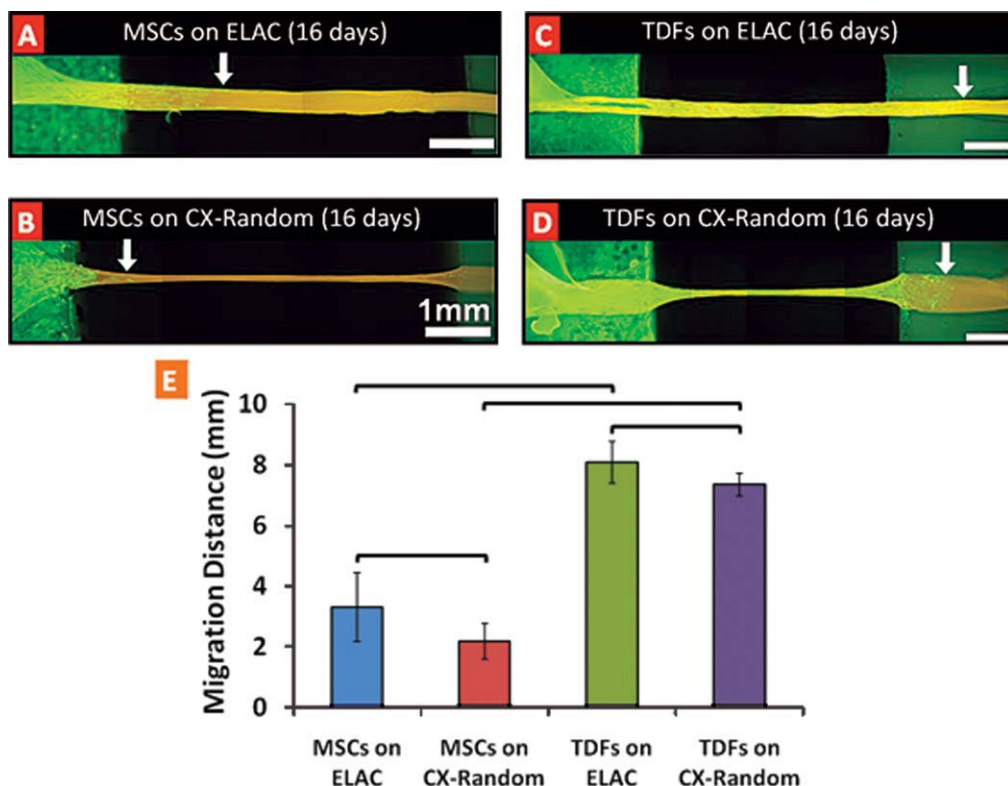


**FIGURE 3.** Migration of MSCs and TDFs on single ELAC and CX-Random collagen bundles. Fluorescent microscope images of typical samples with f-actin filament staining with FITC-Phalloidin (at day-16): (A) MSCs on the ELAC, (B) MSCs on CX-Random, (C) TDFs on ELAC, (D) TDFs on CX-Random. The white arrows indicate the location of the cell migration front. The white scale bars indicate 1 mm distance. (E) Migration distance of MSCs and TDFs on ELAC and CX-Random in 16 days (brackets indicate significant difference between the two groups,  $p < 0.05$ ,  $n = 13-15$ ). [Color figure can be viewed in the online issue, which is available at [www.interscience.wiley.com](http://www.interscience.wiley.com).]

#### Population of 3D ELAC constructs by MSCs and TDFs

Both TDFs [Fig. 6(A)] and MSCs [Fig. 6(B)] can migrate, attach, and populate the 3D braided ELAC constructs. High magnification confocal images showed that the cytoskeletons were organized along the bundle axis direction [Fig. 6(A,B), lower images]. Histological images of transverse cross sections of 3D bundles indicated that TDFs can populate the inter bundle space and attach to the surface of ELAC [Fig. 6(C)]. In the histological images, it is also possible to observe a cell layer detached from the ELAC surface due to histological sample preparation. The presence of such a cell layer indicates that the presence of an extracellular matrix produced by the cells, in which they are embedded.

#### DISCUSSION

The current study investigated the *in vitro* degradation, cytotoxicity, cell migration, and cell morphology of a novel ELAC bundle, which has potential to be used as a biomaterial for tendon/ligament tissue engineering. Two types of cells, TDFs and MSCs were investigated *in vitro*. The key findings of this study were: (1) *In vitro* degradation of ELAC is in the order of weeks, (2) ELAC is not cytotoxic, (3) ELAC is receptive to cell migration, (4) TDFs populated ELAC more readily than MSCs, (5) ELAC does not induce osteogenic phenotype expression by the MSCs, (6) TDFs display a

more anisotropic cytoskeletal orientation along the long axis of the ELAC than MSCs, (7) Both MSC and TDF cytoskeletal fibers are more oriented on ELAC along the long axis than on CX-Random, and (8) The 3D constructs formed by braiding ELAC bundles can be populated by both MSCs and TDFs.

Other researchers have compared tendon/ligament-derived cells and MSCs for tendon/ligament tissue engineering applications. Ge et al.<sup>32</sup> investigated the optimal cell source for anterior cruciate ligament (ACL) tissue engineering. Fibroblasts isolated from ACL, medial collateral ligament (MCL), as well as MSCs were compared. They concluded that MSCs might be better compared to ligament-derived fibroblasts because the cell proliferation rate and collagen excretion of MSCs were higher than those of fibroblasts. Recently, Liu et al.<sup>33</sup> compared rabbit MSCs with anterior cruciate ligament fibroblasts (ACLFs) on a silk scaffold model. Based on the cellular response (ECM production and cell proliferation) *in vitro* and *in vivo*, MSCs were found to be a better cell source than ACLFs for the further study of ACL tissue engineering. Kryger et al.<sup>25</sup> investigated two types of tenocytes (epitenon tenocytes, tendon sheath fibroblasts) and two types of stem cells (MSCs and adipose-derived mesenchymal stem cells (ASCS)) for tendon tissue engineering by using acellularized tendons as scaffold. They found that all cell types had similar collagen expression. Adipose-derived MSCs proliferated faster in cell culture at

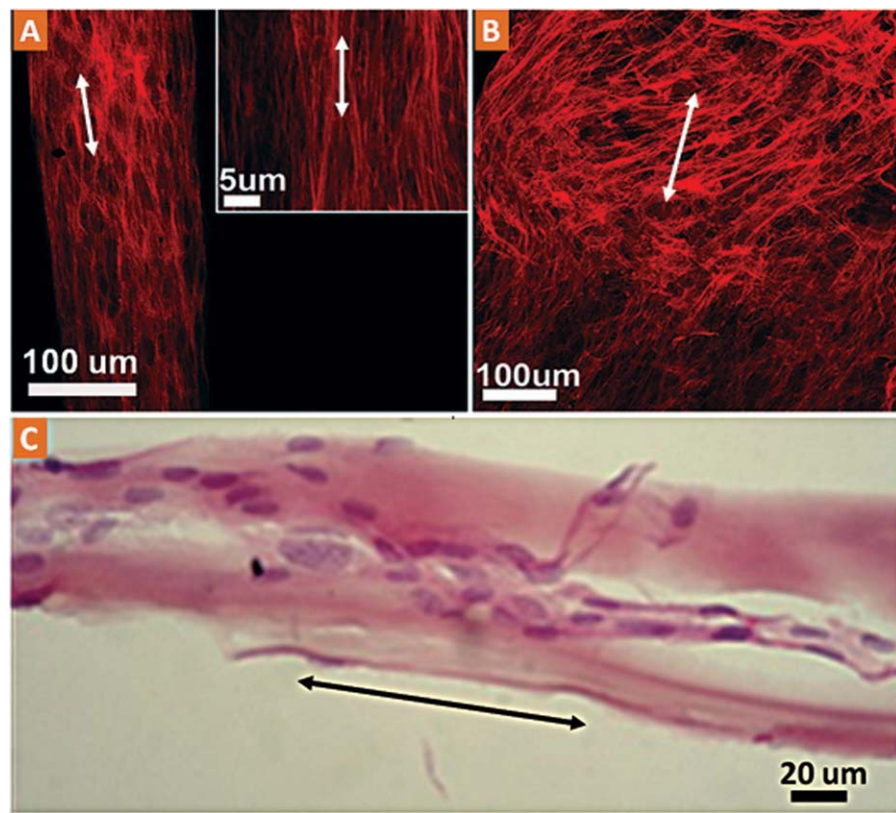


**FIGURE 4.** (A) The high magnification confocal images indicate the dense population and the cytoskeletal alignment of TDFs on ELAC bundles. (B) Confocal microscope images of the CX-Random collagen bundles with the migrated and populated TDFs indicating the random orientation of the cell cytoskeletons. (C) Longitudinal histological section stained with H&E displaying the elongated nuclear morphology. [Color figure can be viewed in the online issue, which is available at [www.interscience.wiley.com](http://www.interscience.wiley.com).]

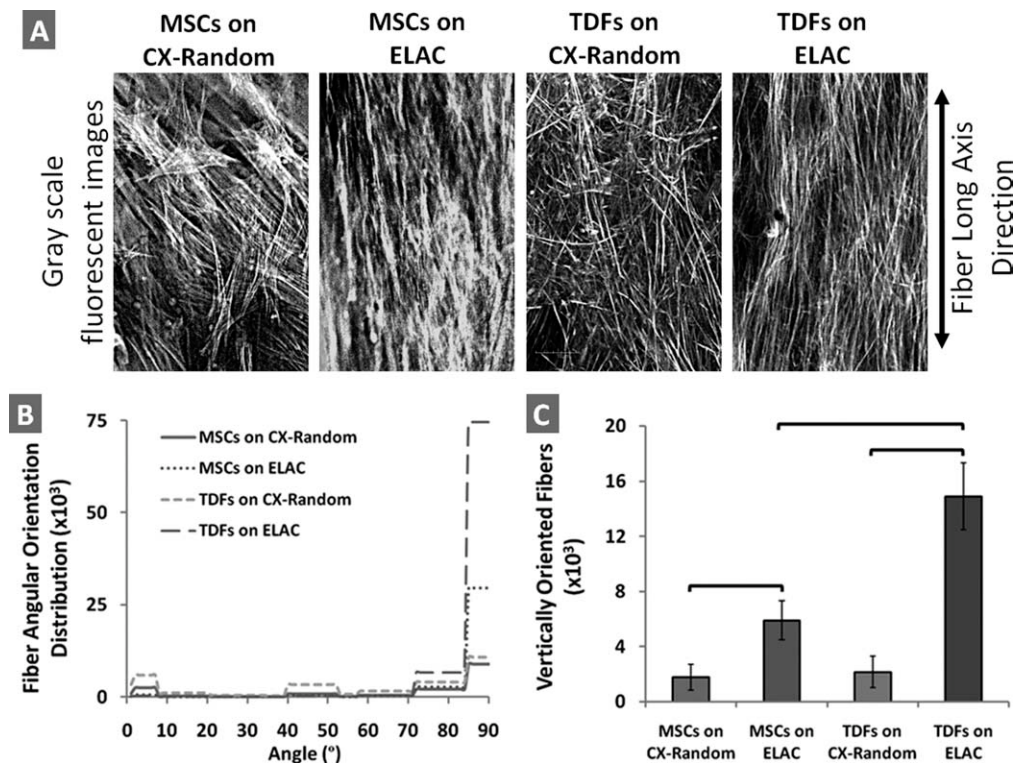


**FIGURE 5.** Quantitative analysis on the cytoskeletal alignment of MSCs and TDFs on ELAC and CX-Random bundles. (A) Gray scale fluorescent images of the cytoskeletal filaments. (B) The distribution of the orientation of cytoskeletal fibrils between 1–90 degrees (data is shown cumulatively with  $n = 5$  for each group). (C) The number of vertically oriented fibers for MSCs and TDFs on ELAC and CX-Random. The brackets indicate statistical significance between the two groups ( $p < 0.05$  with  $n = 5$ ).

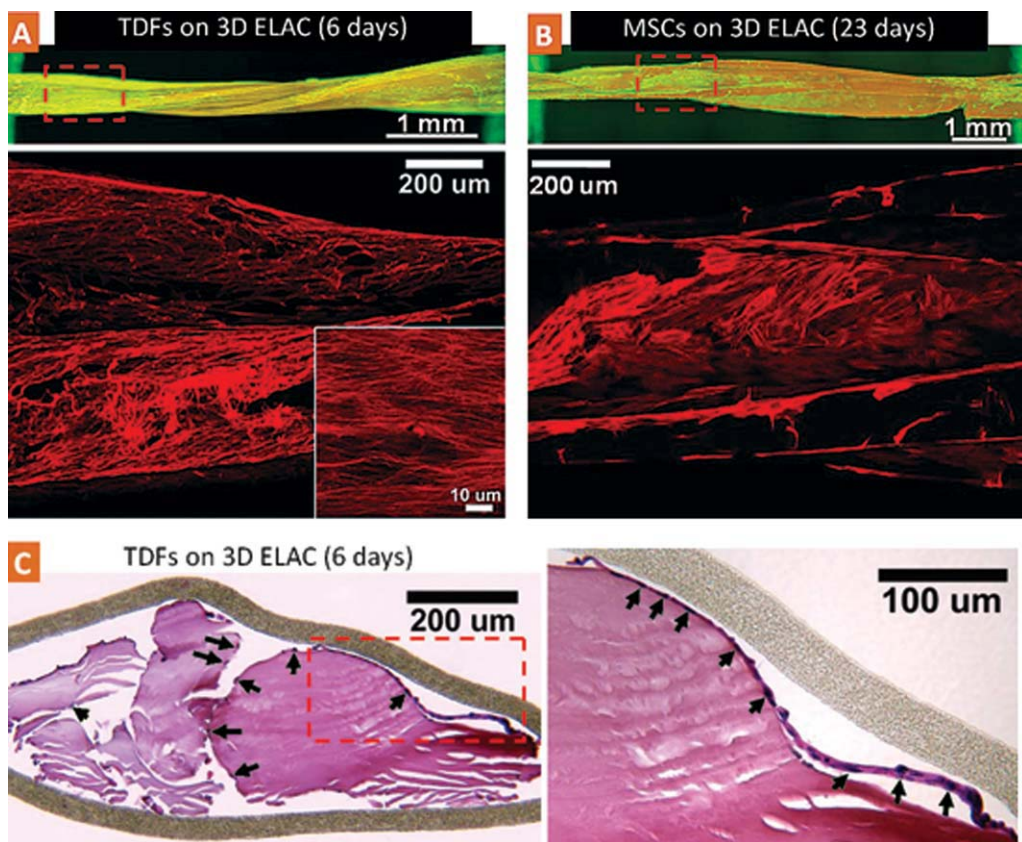


**FIGURE 6.** TDF and MSC population on 3D braided ELAC constructs. (A) Fluorescence and confocal image of TDFs on braided ELAC. The high magnification confocal inset displays the oriented cell cytoskeleton along the collagen fiber direction. (B) Fluorescence and confocal image of MSC populated braided ELAC bundles. (C) Histological (H&E stained) cross-section of braided ELAC bundles populated with TDFs showing that cells (green arrows point the cell nuclei) are attached and populated on the surface of the ELAC bundles. In the higher magnification inset, it is possible to observe a cell layer detached from the ELAC surface due to histological preparation. The presence of such a layer indicates that the cells are able to synthesize an extracellular matrix layer, in which they are embedded. [Color figure can be viewed in the online issue, which is available at [www.interscience.wiley.com](http://www.interscience.wiley.com).]

higher passage numbers, but the cell types were similar in other respects. All cell types were able to successfully populate acellularized tendon *in vitro* as flexor tendon grafts. They suggested that the four cell types may be successfully used to engineer tendons. It appears that MSCs outperform ligament-derived cells whereas tendon-derived cells function comparable to MSCs. In general, stem cells and tissue-derived cell sources have their advantages and disadvantages for tendon/ligament repair. Harvest of MSCs requires access to interior of bones and may include painful biopsies. While, they are easy to expand, passage of MSCs take a long time before usage and they may fail to differentiate into desired phenotype and may lead to ectopic bone formation *in vivo*.<sup>24,32</sup> TDFs, on the other hand, can synthesize neo tendon/ligament tissue readily without induced differentiation. However the cell source is limited and the extraction is more complicated than MSCs. In terms of cell migration, population of ELAC bundles and the cytoskeletal alignment, the current study observed the TDFs to be superior over MSCs.

It is important for cell-scaffold constructs to have sufficient strength after implantation that would allow early

active mobilization, which has been demonstrated to result in effective repair of specific tendon injuries.<sup>34,35</sup> Tendon/ligament tissue engineering also requires the graft biomaterials to be biocompatible and biodegradable. Natural tendon's strong mechanical strength is largely dependent on the aligned Type I collagen matrix. In ELAC material, collagen molecules and fibrils are oriented in parallel as demonstrated by SEM, TEM, and SAXS.<sup>23</sup> Due to close packing, alignment, and crosslinking, the mechanical properties (modulus and strength) of ELAC are comparable to those of tendon.<sup>23</sup> In addition, genipin crosslinked collagenous biomaterials have been shown to be biocompatible *in vivo* and *in vitro* by other studies as well.<sup>36–38</sup> The direct contact test employed in the current study also confirms that there is no toxicity of genipin crosslinked ELAC material and its biodegraded byproducts. Even though it is densely packed and crosslinked, ELAC is still biodegradable and it may allow for cellular remodeling after implantation. Therefore, ELAC seems to carry several of the key qualities of a material that can serve to tissue-engineer replacements of damaged tendon proper.

As the main interest of this study was to compare the population rates of the ELAC and CX-Random collagen

bundles in a macroscopic scale, the cell migration rates were calculated in a similar manner in both of the groups. The cell migration rates were measured along the long axis of the bundles (Fig. 3). Since the cells on CX-Random collagen move randomly (or at least off-axis to the longer axis of the strip) the "net distance" they cover along the longer axis of the construct is shorter. In other words, in terms of cell-guidance along a given direction, ELAC presents advantages. However, the actual rate of cell motility on the two matrices may not have differed should the migration of individual cells be traced.

It has been demonstrated that aligned cells can enhance repair biomechanics during tendon/ligament repair.<sup>22</sup> In tendon, the dense collagen bundles are synthesized by elongated fibroblasts, which are aligned longitudinally along the tendon axis. Migration assays demonstrated that both TDFs and MSCs were able to align along the ELAC fiber axis. The nuclei and cytoskeleton were elongated similar to those of tenocytes *in vivo*. The ability of ELAC to align cells may be explained by contact guidance provided by collagen fibers. Since a single ELAC bundle is about 50–400 µm in diameter and up to several centimeters long, cells can be aligned by contact guidance along the fiber direction.<sup>16</sup> While the individual ELAC bundle is densely packed and does not allow cells to infiltrate, braiding several ELAC bundles together introduces the desired interbundle spacing in the resulting 3D constructs for cellular migration and population. The current results confirmed that such constructs can be populated by MSCs and TDFs. It should be noted that the 3D braided constructs employed in this study was prepared manually. In order to obtain more uniform and comparable braided constructs, the braiding method needs to be automated. The current fabrication method allows synthesis of long ELAC bundles that can be spun on spools and textile machinery can perform the braiding as such in the future.

This study quantified the alkaline phosphatase and osteocalcin activities to assess the osteogenic differentiation state of MSCs and no significant differences were observed between the groups tested. However, there always is a risk for the MSCs to differentiate on stiffer substrates<sup>21,39,40</sup> and the inherent stiffness of ELAC may require additional strategies to reduce the risk of osteogenic differentiation to the minimum possible levels. One strategy to suppress such nonspecific differentiation would be utilization of cytokines, such as BMP-12 which has been previously shown to promote tenogenic differentiation.<sup>41,42</sup> In addition to differentiation of MSCs, proliferation and matrix synthesis of both cell types on ELAC bundles is important and needs further investigation.

In conclusion, genipin crosslinked ELAC has been shown to be nontoxic to cells and biodegradable. Both TDFs and MSCs can migrate onto ELAC bundles and the cell nuclei and cytoskeleton are aligned along the bundle axis, a key morphological similarity to tenocytes *in vivo*. Both cells can populate 3D constructs obtained by braiding multiple ELAC bundles. The above results indicate TDF-ELAC or MSC-ELAC constructs may be suitable candidates as tendon/ligament bioscaffold. Future evaluations of this material will be

directed towards: (1) comprehensive studies on differentiation of MSCs on ELAC bundles, (2) investigation of whether aligned cells on ELAC can synthesize more organized and denser ECMs *de novo* than their counterparts (CX-Random collagen constructs) after implantation, (3) investigation of the biodegradation, remodeling, and biomechanical properties of ELAC constructs *in vivo* using animal models.

## ACKNOWLEDGMENTS

We would like to acknowledge Dr. Edward Bartlett for donating the animals utilized in this study. Any opinions, findings, and conclusions or recommendations expressed in this material are those of the author(s) and do not necessarily reflect the views of the National Science Foundation.

## REFERENCES

- Kofron MD, Laurencin CT. Orthopaedic applications of gene therapy. *Curr Gene Ther* 2005;5:37–61.
- Schoen DC. Injuries of the wrist. *Orthop Nurs* 2005;24:304–307.
- Praemer A, Furner S, Rice D. Musculoskeletal condition in the United States. *Am Acad Orthop Surg*; 1999.
- Butler DL, Juncosa N, Dressler MR. Functional efficacy of tendon repair processes. *Annu Rev Biomed Eng* 2004;6:303–329.
- Koob TJ. Biomimetic approaches to tendon repair. *Comp Biochem Physiol A Mol Integr Physiol* 2002;133:1171–1192.
- Beredjiklian PK. Biologic aspects of flexor tendon laceration and repair. *J Bone Joint Surg Am* 2003;85:539–550.
- Ferretti A, Conteduca F, Camerucci E, Morelli F. Patellar tendinosis: A follow-up study of surgical treatment. *J Bone Joint Surg Am* 2002;84:2179–2185.
- Marder RA, Timmerman LA. Primary repair of patellar tendon rupture without augmentation. *Am J Sports Med* 1999;27:304–307.
- Paavola M, Kannus P, Paakkala T, Pasanen M, Jarvinen M. Long-term prognosis of patients with achilles tendinopathy. An observational 8-year follow-up study. *Am J Sports Med* 2000;28:634–642.
- Krackow KA, Thomas SC, Jones LC. Ligament-Tendon fixation - analysis of a new stitch and comparison with standard techniques. *Orthopedics* 1988;11:909–917.
- Kartus J, Movin T, Karlsson J. Donor-site morbidity and anterior knee problems after anterior cruciate ligament reconstruction using autografts. *Arthroscopy* 2001;17:971–980.
- Kuo YR, Kuo MH, Chou WC, Liu YT, Lutz BS, Jeng SF. One-stage reconstruction of soft tissue and achilles tendon defects using a composite free anterolateral thigh flap with vascularized fascia lata: Clinical experience and functional assessment. *Ann Plastic Surgery* 2003;50:149–155.
- Crossett LS, Sinha RK, Sechrist VF, Rubash HE. Reconstruction of a ruptured patellar tendon with achilles tendon allograft following total knee arthroplasty. *J Bone Joint Surg Am* 2002;84:1354–1361.
- Walton JR, Bowman NK, Khatib Y, Linklater J, Murrell GAC. Restore orthobiologic implant: Not recommended for augmentation of rotator cuff repairs. *J Bone Joint Surg Am* 2007;89:786–791.
- Derwin KA, Baker AR, Spragg RK, Leigh DR, Iannotti JP. Commercial extracellular matrix scaffolds for rotator cuff tendon repair - Biomechanical, biochemical, and cellular properties. *J Bone Joint Surg Am* 2006;88:2665–2672.
- Guilak f, Butler DL, Goldstein SA, Mooney DJ. Functional Tissue Engineering. New York: Springer-Verlag; 2003.
- Chvapil M, Speer DP, Holubec H, Chvapil TA, King DH. Collagen-fibers as a temporary scaffold for replacement of acl in goats. *J Biomed Mater Res* 1993;27:313–325.
- Koob TJ, Willis TA, Hernandez DJ. Biocompatibility of NDGA-polymerized collagen fibers. I. Evaluation of cytotoxicity with tendon fibroblasts in vitro. *J Biomed Mater Res A* 2001;56:31–39.
- Koob TJ, Willis TA, Qiu YS, Hernandez DJ. Biocompatibility of NDGA-polymerized collagen fibers. II. Attachment, proliferation,

- and migration of tendon fibroblasts in vitro. *J Biomed Mater Res* 2001;56:40–48.
20. Fini M, Torricelli P, Giavaresi G, Rotini R, Castagna A, Giardino R. In vitro study comparing two collagenous membranes in view of their clinical application for rotator cuff tendon regeneration. *J Orthop Res* 2007;25:98–107.
  21. Awad HA, Boivin GP, Dressler MR, Smith FNL, Young RG, Butler DL. Repair of patellar tendon injuries using a cell-collagen composite. *J Orthop Res* 2003;21:420–431.
  22. Young RG, Butler DL, Weber W, Caplan AI, Gordon SL, Fink DJ. Use of mesenchymal stem cells in a collagen matrix for Achilles tendon repair. *J Orthop Res* 1998;16:406–413.
  23. Cheng XG, Gurkan UA, Dehen CJ, Tate MP, Hillhouse HW, Simpson GJ, Akkus O. An electrochemical fabrication process for the assembly of anisotropically oriented collagen bundles. *Biomaterials* 2008;29:3278–3288.
  24. Butler DL, Juncosa-Melvin N, Boivin GP, Galloway MT, Shearn JT, Gooch C, Awad H. Functional tissue engineering for tendon repair: A multidisciplinary strategy using mesenchymal stem cells, bioscaffolds, and mechanical stimulation. *J Orthopaedic Res* 2008;26:1–9.
  25. Kryger GS, Chong AKS, Costa M, Pham H, Bates SJ, Chang J. A comparison of tenocytes and mesenchymal stem cells for use in flexor tendon tissue engineering. *J Hand Surg Am* 2007;32:597–605.
  26. Williams BR, Gelman RA, Poppke DC, Piez KA. Collagen fibril formation - optimal invitro conditions and preliminary kinetic results. *J Biol Chem* 1978;253:6578–6585.
  27. Kannus P. Structure of the tendon connective tissue. *Scand J Med Sci Sports* 2000;10:312–320.
  28. Gross CL, Nealley EW, Smith WJ, Corun CM, Nipwoda MT. A rapid colorimetric assay for sulfur mustard cytotoxicity using isolated human peripheral blood lymphocytes and keratinocytes. *Toxicol Mech Methods* 2003;13:263–268.
  29. Cornwell KG, Lei P, Andreadis ST, Pins GD. Crosslinking of discrete self-assembled collagen threads: Effects on mechanical strength and cell-matrix interactions. *J Biomed Mater Res A* 2007;80:362–371.
  30. Canny J. A Computational Approach to Edge-Detection. *IEEE Trans Pattern Anal Mach Intell* 1986;8:679–698.
  31. Maccarinelli G, Sibilia V, Torsello A, Raimondo F, Pitto M, Giustina A, Netti C, Cocchi D. Ghrelin regulates proliferation and differentiation of osteoblastic cells. *J Endocrinol* 2005;184:249–256.
  32. Ge Z, Goh JC, Lee EH. Selection of cell source for ligament tissue engineering. *Cell Transplant* 2005;14:573–583.
  33. Liu HF, Fan HB, Toh SL, Goh JCH. A comparison of rabbit mesenchymal stem cells and anterior cruciate ligament fibroblasts responses on combined silk scaffolds. *Biomaterials* 2008;29:1443–1453.
  34. Silfverskiold KL, May EJ, Oden A. Factors affecting results after flexor tendon repair in zone.2. A multivariate prospective analysis. *J Hand Surg Am* 1993;18:654–662.
  35. Becker H, Orak F, Duponselle E. Early active motion following a beveled technique of flexor tendon repair: Report on fifty cases. *J Hand Surg Am* 1979;4:454–460.
  36. Chang Y, Tsai CC, Liang HC, Sung HW. In vivo evaluation of cellular and acellular bovine pericardia fixed with a naturally occurring crosslinking agent (genipin). *Biomaterials* 2002;23:2447–2457.
  37. Chen YS, Chang JY, Cheng CY, Tsai FJ, Yao CH, Liu BS. An in vivo evaluation of a biodegradable genipin-cross-linked gelatin peripheral nerve guide conduit material. *Biomaterials* 2005;26:3911–3918.
  38. Huang LLH, Sung HW, Tsai CC, Huang DM. Biocompatibility study of a biological tissue fixed with a naturally occurring crosslinking reagent. *J Biomed Mater Res* 1998;42:568–576.
  39. Harris MT, Butler DL, Boivin GP, Florer JB, Schantz EJ, Wenstrup RJ. Mesenchymal stem cells used for rabbit tendon repair can form ectopic bone and express alkaline phosphatase activity in constructs. *J Orthop Res* 2004;22:998–1003.
  40. Nirmalanandhan VS, Juncosa-Melvin N, Shearn JT, Boivin GP, Galloway MT, Gooch C, Bradica G, Butler DL. Combined effects of scaffold stiffening and mechanical preconditioning cycles on construct biomechanics, gene expression, and tendon repair biomechanics. *Tissue Eng A* 2009;15:2103–2111.
  41. Violini S, Ramelli P, Pisani LF, Gorni C, Mariani P. Horse bone marrow mesenchymal stem cells express embryo stem cell markers and show the ability for tenogenic differentiation by in vitro exposure to BMP-12. *BMC Cell Biol* 2009;10:29.
  42. Li Y, Ramcharan M, Fung DT, Majeska RJ, Schaffler MB, Flatow EL, Sun HB. BMP-12 Selectively Induces Differentiation of Human Mesenchymal Stem Cells (MSCs) to a Tenocyte-like Phenotype. The 55th Annual Meeting of Orthopaedic Research Society, Las Vegas, NV: 2009.